Journal of Colloid and Interface Science 518 (2018) 48–56

Contents lists available at ScienceDirect

Journal of Colloid and Interface Science

journal homepage: www.elsevier.com/locate/jcis

Regular Article

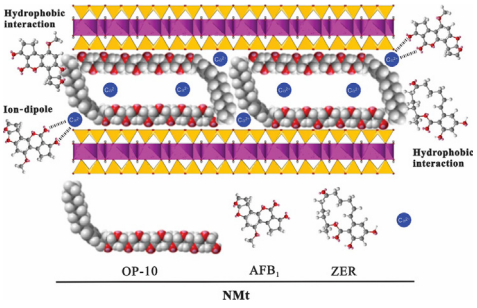
Evaluation of nonionic surfactant modified montmorillonite as mycotoxins adsorbent for aflatoxin B_1 and zearalenone

Gaofeng Wang [a,b], Chi Lian [a], Yunfei Xi [b], Zhiming Sun [a,*], Shuilin Zheng [a,*]

[a] School of Chemical and Environmental Engineering, China University of Mining and Technology (Beijing), Beijing 100083, China
[b] School of Earth, Environmental and Biological Sciences, Science and Engineering Faculty, Queensland University of Technology (QUT), 2 George Street, Brisbane, QLD 4001, Australia

GRAPHICAL ABSTRACT

Polar mycotoxin AFB_1 can be captured by the exchangeable cations through ion-dipole interactions and the organic carbon chains through hydrophobic interaction. Low polar, hydrophobic mycotoxin ZER was mainly adsorbed through hydrophobic interaction.



ARTICLE INFO

Article history:
Received 9 January 2018
Revised 5 February 2018
Accepted 5 February 2018
Available online 7 February 2018

Keywords:
Mycotoxins adsorbent
Montmorillonite
Nonionic surfactant
Aflatoxin B_1
Zearalenone

ABSTRACT

This work aims at exploring the potential of nonionic surfactant octylphenol polyoxyethylene ether (OP-10) modified montmorillonites (NMts) as mycotoxins adsorbent. The resulting NMts has different structural configurations, organic carbon contents, surface hydrophobicity and textural properties at different surfactant loadings. The prepared NMts were used for adsorption of polar aflatoxin B_1 (AFB_1) and weak polar zearalenone (ZER) in both single and binary-contaminate systems by simulating conditions of gastrointestinal tract. The adsorption capacities of NMts to AFB_1 and ZER increased up to 2.78 and 8.54 mg/g respectively from 0.51 and 0.00 mg/g of raw montmorillonite (Mt). High adsorption capacities of NMts to AFB_1 and ZER could be reached at low surfactant loadings. There was little decrease from pH of 3.5 to 6.5 but became negligible with increasing the surfactant loadings. In binary-contaminate adsorption system, the adsorption of ZER was obviously affected by the existence of AFB_1, while ZER had little effect on the adsorption process of AFB_1 due to different adsorption mechanism. This study demonstrates that NMts could be a promising adsorbent for simultaneous detoxification of polar and non-polar mycotoxins.

© 2018 Elsevier Inc. All rights reserved.

1. Introduction

The worldwide contamination of animal feeds, cereal grains and foods intended for human consumption with mycotoxins has been a long-lasting significant problem [1]. It has been estimated that

* Corresponding authors.
E-mail addresses: zhimingsun@cumtb.edu.cn (Z. Sun), zhengsl@cumtb.edu.cn (S. Zheng).

https://doi.org/10.1016/j.jcis.2018.02.020
0021-9797/© 2018 Elsevier Inc. All rights reserved.

almost 25% of food crops over the world are contaminated with mycotoxins each year [2–4]. Mycotoxins are a large group of secondary metabolic products from fungi, or molds, which pose huge health threat to animals and humans due to their mutagenicity and carcinogenicity [5,6]. Moreover, mycotoxins bring enormous economic losses in food industry and animal husbandry annually. Thus, strategies to eliminate or inactivate mycotoxins in foods and feeds which are highly toxic to human and animals remain a research priority.

Several techniques including biological degradation, extrusion cooking, ammoniation and ozonation have been developed for the treatment of mycotoxins [7,8]. However, they have some limitations such as low efficacy, long time treatment, losses in the nutritional value and the palatability of feeds, as well as the expensive equipment required to implement these techniques. Using mycotoxins adsorbents to bind mycotoxins in gastrointestinal tract of animals and then decrease their bioavailability and toxicities has been regarded as the most promising and economical approach to detoxifying mycotoxins contaminated animal feedstuffs [9,10]. Recent studies applying zeolite [11], montmorillonite [12,13], halloysite [14], talc and diatomite [15] for detoxification of mycotoxins suggest the potential of natural minerals as mycotoxins adsorbents. Of particular note in the regard is montmorillonite (Mt), an aluminum silicate possessing a permanent negatively charged surface and exchangeable cations in the interlayer space. Reports show that Mt has excellent effectiveness in binding polar aflatoxins and reducing their toxicity [16–21]. However, the hydrophilic negatively charged surface of Mt is less effective in binding low polar, hydrophobic mycotoxins such as zearalenone and ochratoxin [7,11].

Organic modification of clay minerals with cationic surfactant is another strategy to improve the affinity of adsorbents to non-polar or weak polar mycotoxins. Unfortunately, few studies can be founded for the detoxification of polar aflatoxins using organic clay to the best of our knowledge. Simultaneous detoxification of mycotoxins with different polarities remains a critical unmet challenge.

More recently some groups have explored amphiphilic surfactants such as nonionic and zwitterionic surfactants for simultaneous adsorption of hydrophilic heavy metal ions and hydrophobic organics [22–25]. These pioneering studies give us new inspiration of utilizing amphiphilic surfactants to modify Mt for simultaneous adsorption of mycotoxins with different polarities. Despite the popularity of amphiphilic surfactant modified Mts used in environmental recommendation, no studies have yet successfully applied amphiphilic surfactant modified Mts as mycotoxins adsorbents for the simultaneous detoxification of different kind of mycotoxins.

Here we use the nonionic surfactant octylphenol polyoxyethylene ether with 10 CH_2CH_2O radicals (OP-10) as a modifier to develop a novel Mt-based mycotoxins adsorbent (NMt). The structure configurations and organic contents of NMts were detected with XRD and TG techniques. The surface hydrophobicity was deduced from moisture adsorption capacity. And the porous nature of NMts was measured from N_2 adsorption–desorption isotherms. The potential of NMt as mycotoxins adsorbent was examined with the adsorption properties of polar aflatoxin B_1 (AFB_1) and weak polar zearalenone (ZER). The molecular structures of AFB_1 and ZER are displayed in Fig. 1, the dipole moment of which is 9.5 and 2.2 D, respectively.

2. Materials and methods

2.1. Materials

The montmorillonite (Mt) with a cation exchange capacity (CEC) of 68.29 meq/100 g used in this study is supported by Baifubang Mining Fertilizer Co. Ltd. from Neimenggu province, China. It was ground into powder to pass through 200 mesh after being received. It contains very little quartz but no organic matter. And no excess hazardous heavy metals and dioxin are detected too in raw Mt, which meets the requirements of feed additives. The nonionic surfactant used in this study is octylphenol polyoxyethylene ether (OP-10) obtained from Usolf Chem. Co., China with a purity of 99%. Mycotoxins aflatoxins B_1 (AFB_1) and zearalenone (ZER) were purchased from Fermentek Co. Ltd, whose purity is above 99.5% analyzed by HPLC method. Other chemical reagents such as phosphoric acid, sodium phosphate monobasic, disodium phosphate, acetonitrile and methyl alcohol were all purchased from Beijing Reagent Co. (Beijing, China). Acetonitrile and methyl alcohol are chromatographic grade, and other reagents are analytical grade. All reagents are used as obtained without further purification.

2.2. Preparation of NMts

The NMts were prepared using an ultrasonic bath method. Firstly, 4 g of Mt was dispersed in 300 mL of deionized water and stirred 0.5 h to form a homogeneous clay dispersion at room temperature. A stoichiometric amount of surfactants were firstly dissolved in 100 mL of deionized water and then slowly introduced to the clay suspension using a peristaltic pump. The mixtures were treated for 0.5 h at 60 °C on a Geneng G-020 ultrasonic bath with ultrasonic power of 120 W and frequency of 40 kHz, and then stirred for another 24 h at room temperature with a Kexi magnetic

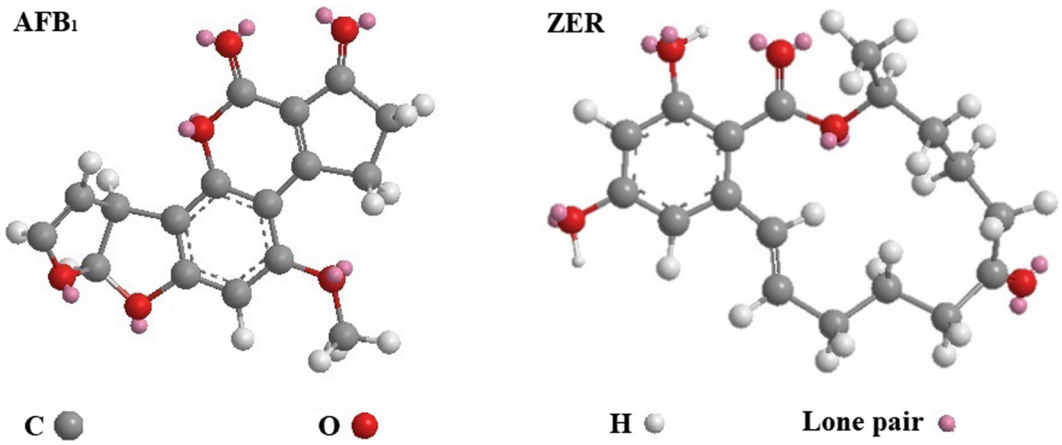


Fig. 1. Molecular structural information of AFB_1 (polar mycotoxin, dipole moment: 9.5 D) and ZER (weak polar mycotoxin, dipole moment: 2.2 D).

stirrer. Finally, the mixtures were washed three times with deionized water by centrifuging for 25 min at 3000 rpm, and then dried in an oven at 60 °C for 12 h. The amounts of surfactants added were 0.5, 1.0 and 2.0 CEC of Mt, which were denoted as 0.5OP-10Mt, 1.0OP-10Mt and 2.0OP-10Mt, respectively.

2.3. Characterization of NMts

Powder X-ray diffraction (XRD) patterns were recorded between 2° and 12° on a Bruker D8 diffractometer with Cu Kα radiation (λ = 0.15406 nm) operating at 40 kV and 40 mA at a step size of 0.02.

Thermogravimetric analysis (TGA) was obtained using a Mettler TGA/DSC 1 SF/1382 instrument with heating rate at 10 °C/min from room temperature to 1000 °C in a high-purity nitrogen atmosphere (50 mL/min).

The hydrophobicity of NMts was deduced from the moisture adsorption experiments under 20 °C with the relative humidity of 33%. The experiments were operated in a GDW-300 programmable temperature and humidity test chamber. All samples were dried at 105 °C for 24 h before the tests were conducted. The moisture adsorption capacities were calculated from the change in mass of samples by the equation:

$$Ma = \frac{m_t - m_0}{m_0} \times 100\%$$

where *Ma* is moisture content, m_0 is the initial weight of the dried sample, and m_t is the weight of the sample at time *t*.

Pore structure parameters such as surface area, pore volume and average pore size were measured from N_2 adsorption–desorption isotherms using a Micromeritics ASAP2020 instrument. The samples were degassed at 105 °C for 12 h prior to N_2 adsorption.

2.4. Simulated mycotoxins adsorption experiments

The mycotoxins adsorption experiments simulated the pH conditions in the gastrointestinal tract using phosphate buffer solutions, at pH 3.5 which is equivalent to stomach and at pH 6.5 which is equivalent to intestine conditions [26]. The experiments were carried in a batch model and performed at 37 °C. Two adsorption systems, namely single adsorption system and binary-contaminant adsorption system, were designed to investigate the adsorption properties of the prepared adsorbents for AFB_1 and ZER. For single adsorption system, only one mycotoxin with an initial concentration of 0.786–3.368 mg/L for AFB_1 or 5.000–14.000 mg/L for ZER, respectively was added into the adsorption system. The pH of phosphate buffer solution was adjusted to 3.5 by adding small amounts of 0.1 M H_3PO_4. For binary-contaminant adsorption system, the adsorption contained both AFB_1 and ZER simultaneously. The initial concentration was set as a constant of 4.000 mg/L for AFB_1 and 16.000 mg/L for ZER, respectively.

Batch adsorption experiments were operated in sealed 25 mL polypropylene centrifuge tubes. Initially, a primary AFB_1 (22.450 mg/L) and ZER (100.000 mg/L) stock solution was prepared by dissolving mycotoxins powders in chromatographic grade methyl alcohol. Then, 0.01 g of the prepared adsorbents as well as raw Mt were added into 10 mL aliquots of phosphate-buffered solution containing AFB_1 or/and ZER at different initial concentrations, respectively. The mixture was continuously agitated on a shaker for 60 min, centrifuged for 5 min at 10,000 rpm, and 1 mL of the aqueous supernatant was filtered with 0.22 μm filter membrane for HPLC analysis. Moreover, a control treatment without adsorbent was carried out for each experiment in case of any possible nonspecific binding of AFB_1 and ZER. All adsorption experiments in this paper were carried out at least in triplicate and the averaged values were presented in the figures. Error bars represent standard deviation of at least three independent experiments. The experiments of raw Mt were performed five replicates due to low adsorption capacity, others were performed in triplicate.

HPLC analyses were performed on an Agilent 1260 quaternary pump with a G1329A autosampler and a welchrom 4.6 × 250 mm XB-C18 column. Isocratic elution was performed with a fluorescence detector at an excitation of 360 nm and an emission of 440 nm for AFB_1, an excitation of 274 nm and an emission of 440 nm for ZER. The mobile phase water and acetonitrile (v/v = 50:50) was pumped at a flow rate of 1.0 mL/min. Calibration curves were achieved using eight standards over the concentration range of the sorption samples and repeated for three times. The adsorbed amount (%) of AFB_1 and ZER was calculated from the difference of the peak area between control supernatant and equilibrium supernatant:

$$R = \left(1 - \frac{A_1}{A_0}\right) \times 100\% \quad (1)$$

where A_0 and A_1 are the peak area of control supernatant and equilibrium supernatant analyzed by HPLC method.

3. Results and discussion

3.1. Characterizations

The XRD patterns of the prepared NMts modified at different surfactant loadings as well as raw Mt were presented in Fig. 2. In Fig. 2, raw Mt has a basal spacing of 1.41 nm, which is typical basal spacing at Ca^{2+} saturation of exchange sites of Mt. After modification with OP-10, d_{001} values of NMts increased with surfactant loadings, which indicated that nonionic surfactant OP-10 has been intercalated into the interlayer of Mt. Being different from cationic surfactant, nonionic surfactant is absent of cations in the molecular structure and therefore no ion exchange reaction occurred between exchangeable cations of Mt and nonionic surfactant. However, literatures reported that hydrogen bond can be formed between polyoxyethylene ether chain and siloxane surfaces [27–31], which supported that nonionic surfactant OP-10 can be

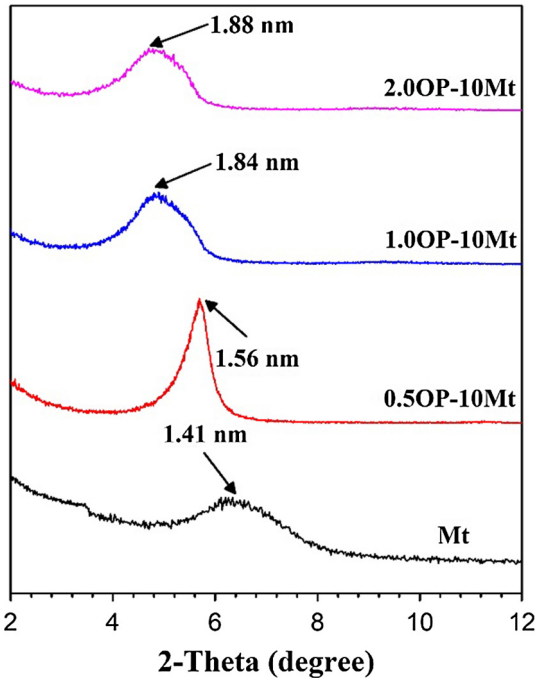


Fig. 2. X-ray diffraction patterns of raw Mt and the prepared NMts modified at 0.5, 1.0 and 2.0 CEC surfactant loadings.

intercalated into the interlayer of Mt through hydrogen bonding. The structural configuration of surfactant molecules between clay unit layers were proposed based on the interlayer spacing and molecular size of OP-10, and the results were discussed systematically somewhere else [32]. At a low surfactant loading (0.5 CEC), OP-10 molecules exhibited a lateral-monolayer arrangement within the interlayer space of Mt. At 1.0 and 2.0 CEC levels, a bilayer arrangement of the surfactant OP-10 could be observed in the interlayer of the clay.

The TG curves of untreated Mt and NMts at different surfactant loadings were displayed in Fig. 3. It was observed from Fig. 3, raw Mt had three main mass loss steps, which were attributed the dehydration of adsorbed water, water molecules around metal cations on the exchangeable sites in Mt and the dehydroxylation of structural OH units in the clays [33,34], respectively. The amount of physically adsorbed water of raw Mt was relatively high, reaching around 11% of total mass of Mt. However, the first mass loss step of NMts, which was assigned to the dehydration of physically adsorbed water, dropped only a little compared to raw Mt. This result demonstrated that the hydrophobicity of NMts increased after modification since partial adsorbed water molecules were replaced by OP-10 molecules. The second mass loss step during approximately 200 to 500 °C, which represented the decomposition of the surfactant, increased from 7.40% to 28.66% when the surfactant loading increased from 0.5 to 2.0 CEC. It indicated the high organic carbon contents of NMts. Though some carbon residue might remain during TGA process [32], the mass losses of NMts were significant.

The surface hydrophobicity was an important property of NMts during nonpolar, hydrophobic contaminants adsorption process. The surface hydrophobicity of NMts was visualized in Fig. 4. The moisture adsorption capacities dropped from 11.82% of raw Mt to 5.32%, 4.33% and 3.33% of 0.5OP-10Mt, 1.0OP-10Mt and 2.0OP-10Mt, respectively, indicating the increase of hydrophobicity of NMts. The results were in good accordance with TG curves, and the increased hydrophobicity of NMts is inclined to capture the nonpolar, hydrophobic molecules.

Fig. 5 displayed the nitrogen adsorption–desorption isotherms of raw Mt and NMts. It can be seen from Fig. 5 that the adsorption–desorption isotherms gradually changed from Type IV of raw Mt to Type II of 1.0OP-10Mt and 2.0OP-10Mt according to the BDDT classification [35]. The Type IV isotherm of raw Mt is characteristic of mesoporous material, meaning the presence of mesopores in raw Mt. However, Type II isotherms of 1.0OP-10Mt and 2.0OP-10Mt suggested nonporous or macroporous adsorbents.

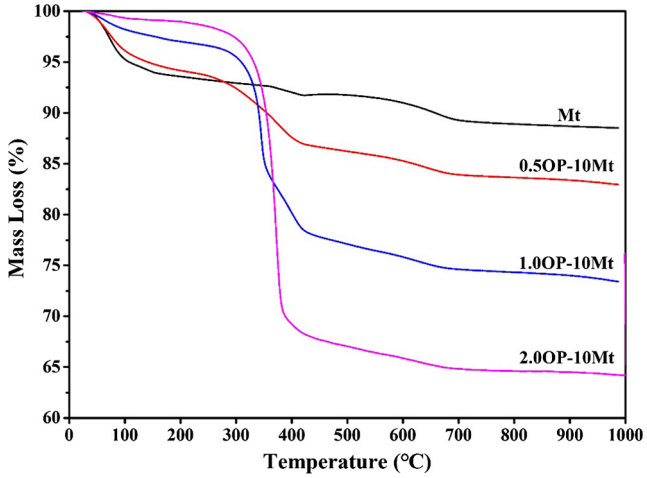


Fig. 3. TG curves of raw Mt and the prepared NMts modified at 0.5, 1.0 and 2.0 CEC surfactant loadings.

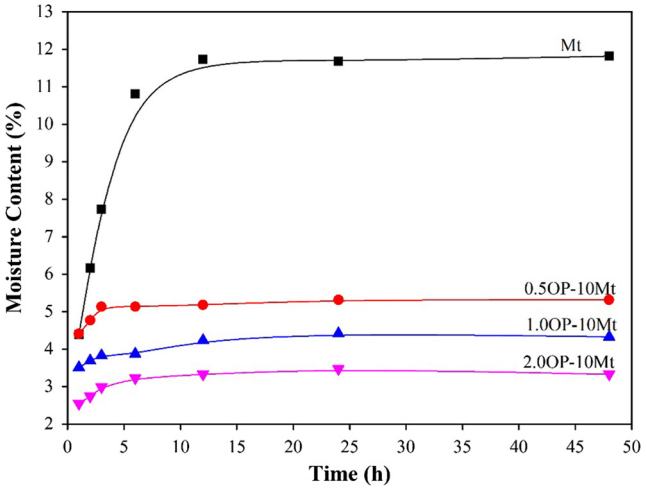


Fig. 4. Moisture adsorption capacities of raw Mt and the prepared NMts modified at 0.5, 1.0 and 2.0 CEC surfactant loadings.

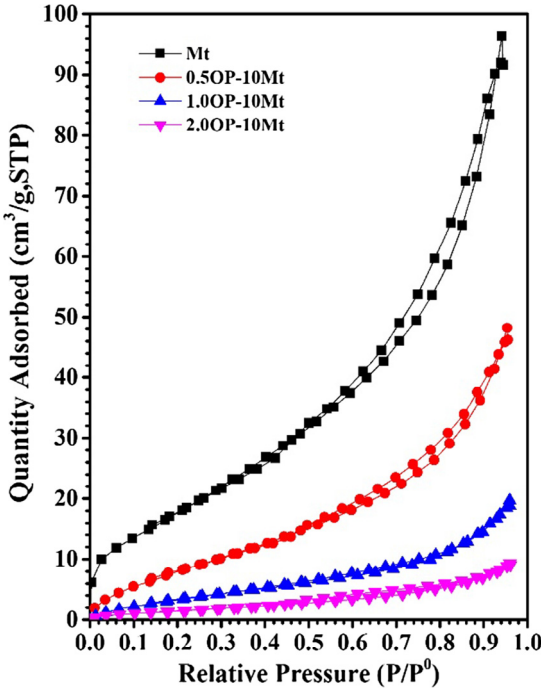


Fig. 5. Nitrogen adsorption–desorption isotherms of raw Mt and the prepared NMts modified at 0.5, 1.0 and 2.0 CEC surfactant loadings.

Table 1
The textural characteristics of raw Mt and the prepared NMts.

Sample ID	S_{BET}[a] (m^2/g)	V_P[b] (cm^3/g)	Pore size[c] (nm)
Mt	72.301	0.170	6.538
0.5OP-10Mt	36.967	0.087	6.327
1.0OP-10Mt	15.920	0.035	6.423
2.0OP-10Mt	6.460	0.017	6.072

[a] S_{BET} means specific surface areas calculated from BET theory.
[b] V_P means BJH desorption cumulative pore volume of pores between 1.7 and 300 nm in diameter.
[c] Pore size is BJH desorption average pore size (4V/A).

Combined with the finding that the BET specific surface area of NMts kept dropping with increasing the surfactant loadings (summarized in Table 1), which may be occupied by the surfactant

molecules. We regarded that the NMts modified at high surfactant loadings are probably nonporous materials. The BET specific surface area and BJH desorption cumulative pore volume sharply declined from 72.301 m^2/g and 0.170 cm^3/g of raw Mt to 6.460 m^2/g and 0.017 cm^3/g of 2.0OP-10Mt, which demonstrated the great changes in textural properties of NMts after modification with nonionic surfactant.

3.2. Adsorption in single system

3.2.1. Adsorption of AFB_1

In order to investigate the adsorption characteristics of the prepared adsorbents, three typical adsorption isotherm models including Langmuir, Freundlich and Linear isotherm models were applied to fit the experimental data. It is assumed that Langmuir isotherm model follows a monolayer adsorption process, which means no further adsorption occurs once adsorbate takes place at specific sites in the adsorbent. The relationship is expressed as follows:

$$\frac{c_e}{q_e} = \frac{1}{q_m} c_e + \frac{1}{q_m K_L} \quad (2)$$

where q_e is the equilibrium adsorption capacity (mg/g), c_e represents the equilibrium concentration in solution (mg/L), K_L is the Langmuir constant (L/mg) and q_m represents the maximum adsorption capacity of the adsorbent (mg/g). Experimental values of q_m and K_L are calculated from the slope and intercept of the linear plot of c_e/q_e against c_e.

On the other hand, the Freundlich model is an empirical expression, which assumed that a multilayer adsorption occurs on the heterogeneous surface or surface supporting sites of various affinities [36]. The equation is described as follows:

$$\ln q_e = \frac{1}{n} \ln c_e + \ln K_F \quad (3)$$

where K_F and $1/n$ are the Freundlich constants which represent the adsorption capacity and adsorption strength, respectively. The magnitude of $1/n$ quantifies the degree of heterogeneity of the adsorbent surface and the favorability of adsorption [37]. K_F and n can be obtained from the intercept and slope of the linear plot of ln q_e versus ln c_e.

The linear isotherm model can be expressed as:

$$q_e = K_d c_e \quad (4)$$

where q_e is the solid-phase concentration of the sorbate per unit mass of the sorbent (mg/g), c_e is the equilibrium solute concentration (mg/L), and K_d is the linear sorption (partition) coefficient (L/g).

Fig. 6 showed the adsorption isotherms of raw Mt and the prepared adsorbents NMts to AFB_1. The relevant parameters of the three isotherm models were calculated in Table 2. Seen from Table 2, the experimental data of raw Mt matched best with Freundlich model based on the correlation coefficients (R^2), suggesting that either the presence of a heterogeneous sorbent surface or the co-existence of different adsorption mechanism, or both phenomena at the same time [38]. It was generally considered that the exchangeable cations of Mt were the main sorption sites of AFB_1. Ion-dipole interaction and coordination happened between the cations of Mt and carbonyl groups of AFB_1 [6,39,40]. However, raw Mt had a very low adsorption capacity to AFB_1, 0.51 mg/g actually obtained in this study. Moreover, the adsorption affinity between AFB_1 and raw Mt is weak observed from the value of dimensionless parameter 1/n (1/n > 1) [6].

The adsorption isotherms of NMts to AFB_1 could be best described by Langmuir model seen from Table 2 ($R^2 > 0.99$), indicating different sorption sites for AFB_1 between raw Mt and NMts. On the basis of Langmuir model, the adsorption of AFB_1 on NMts obeyed monolayer adsorption process and the monolayer maximum adsorption capacities of 0.5OP-10Mt, 1.0OP-10Mt and 2.0OP-10Mt were 2.78, 2.69 and 2.72 mg/g, respectively. It was reported that one nearly-planar AFB_1 molecule occupied about 1.38 nm^2 surface area [41]. We calculated that the 2.78, 2.69 and 2.72 mg/g adsorption capacities of 0.5OP-10Mt, 1.0OP-10Mt and 2.0OP-10Mt required a surface area of 7.41, 7.17 and 7.25 m^2/g at monolayer adsorption, respectively. The specific surface areas of 0.5OP-10Mt, 1.0OP-10Mt and 2.0OP-10Mt were 36.967, 15.920 and 6.460 m^2/g, respectively as mentioned in Table 1. It was clear that 0.5OP-10Mt, 1.0OP-10Mt could provide enough sorption sites for AFB_1 but the specific surface area of 2.0OP-10Mt is lower than the required sorption sites. The lower specific surface area of 2.0OP-10Mt than required sorption site reminded the existence of ion-dipole interaction and coordination between cations of NMts and carbonyl groups of AFB_1, since OP-10 molecules didn't replace the exchangeable cations of Mt. It was interesting that the sorption sites of 0.5OP-10Mt increased obviously as compared to raw Mt but kept almost constant among the three prepared NMts. The finding showed that though the surfactant loadings of 0.5OP-10Mt, 1.0OP-10Mt and 2.0OP-10Mt were different, the

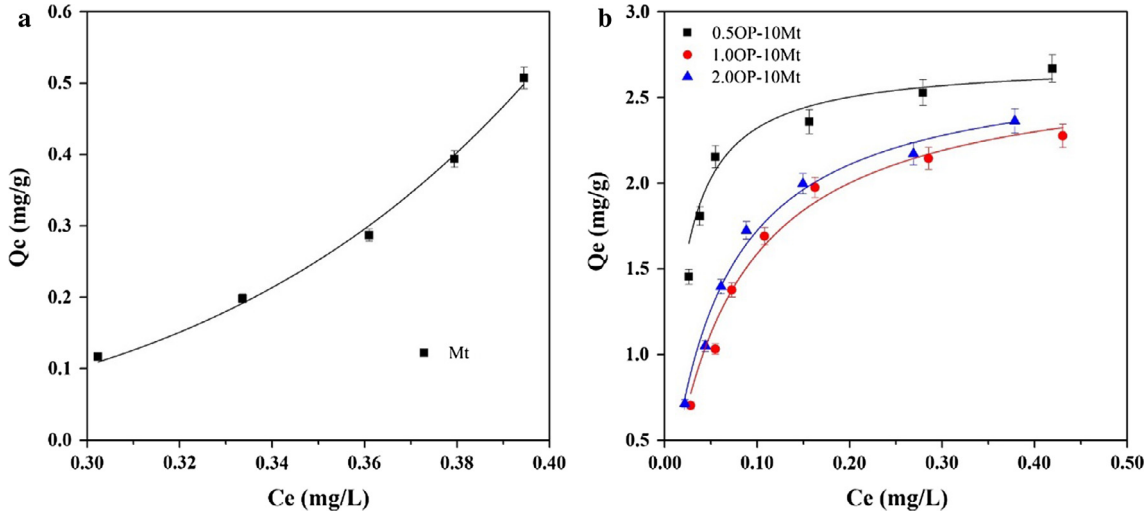


Fig. 6. Adsorption isotherms of (a) Mt, (b) 0.5OP-10Mt, 1.0OP-10Mt and 2.0OP-10Mt to AFB_1. The data points are the average values of repeat experiments. The error bars represent standard deviation of the replicates. The raw Mt was performed five replicates due to low adsorption capacity, others were performed in triplicate.

Table 2
The parameters of isotherm models for AFB_1 adsorption.

AFB_1	Langmuir model			Freundlich model			Linear model	
	Q_{max} (mg/g)	K_L (L/mg)	R^2	K_F ($mg^{1-1/n}L^{1/n}/g$)	1/n	R^2	K_d	R^2
Mt	0.05	2.33	0.9713	100.74	5.71	0.9946	4.10	0.9511
0.5OP-10Mt	2.78	44.99	0.9989	3.27	0.19	0.8672	2.50	0.7412
1.0OP-10Mt	2.69	13.65	0.9954	3.81	0.43	0.9103	3.49	0.7458
2.0OP-10Mt	2.72	16.62	0.9972	3.96	0.41	0.9220	4.03	0.7780

sorption sites they can provide for AFB_1 were almost the same. We ascribed this to the structural configuration of surfactant molecules between clay mineral unit layers at different surfactant loadings. As demonstrated in Fig. S1, when the hydrophobic carbon chain of OP-10 acted as the sorption sites for AFB_1, the effective sorption sites of NMts modified at different surfactant loadings were almost the same. Thus, we inferred that the hydrophobic carbon chain of OP-10 should be the created sorption sites of the new adsorbents. In this case, hydrophobic interaction between carbon chain and organic parts of AFB_1 would dominate the adsorption process of AFB_1 on NMts, assisted with ion-dipole interaction and coordination.

Combined with the configuration of NMts proposed in literature [32], we speculated that NMts modified between 0.5 and 1.0 CEC level which had higher effective sorption sites could own a higher adsorption capacity. In order to verify the speculation, 0.75OP-10Mt modified at 0.75 CEC surfactant loading was prepared, characterized and applied in the adsorption of AFB_1. XRD pattern (shown in Fig. S2a) implied the interlayer spacing of 0.73 nm, which reflected a paraffin-type monomolecular arrangement (Fig. S2b). TG and BET measurements gave organic carbon content and specific surface area of 13.81% and 21.587 m^2/g (Fig. S2c and d), which was between 0.5OP-10Mt and 1.0OP-10Mt. The comparative adsorption result from 0.5 to 2.0 CEC OP-10 modified samples was illustrated in Fig. S3. It showed that 0.75OP-10Mt had the highest adsorption capacity, which confirmed the speculation. Therefore, we concluded that NMt could reach high adsorption capacities under low surfactant loadings, thereby having lower production cost and wide application prospect.

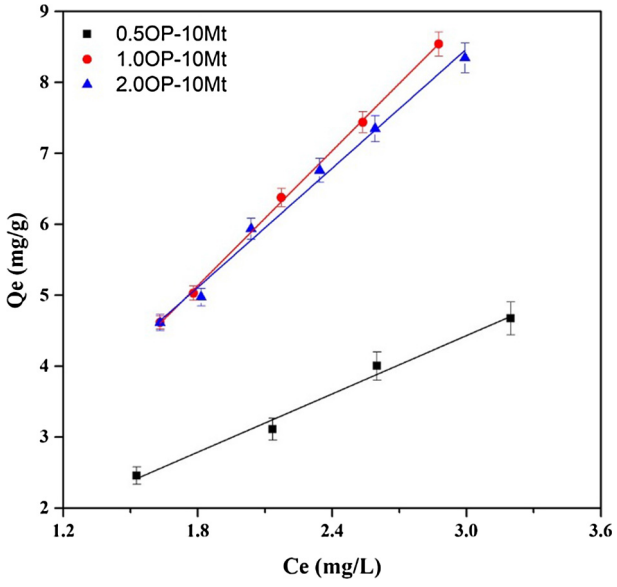


Fig. 7. Adsorption isotherms of 0.5OP-10Mt, 1.0OP-10Mt and 2.0OP-10Mt to ZER. The data points are the average values of repeat experiments. The error bars represent standard deviation of three replicates.

3.2.2. Adsorption of ZER

The adsorption isotherms of NMts for ZER were displayed in Fig. 7. However, the adsorption isotherm of raw Mt was not plotted because our experimental data found that raw Mt hardly adsorbed ZER in the simulated gastrointestinal tract solution due to the hydrophilic, strong polar surface of Mt against the hydrophobic, weak polar ZER molecules. It can be seen clearly from Fig. 7 that the adsorption capacities of NMts for ZER were dramatically enhanced after modification and the adsorption isotherms of NMts could be described well with Linear model. The result was later proved by the calculated parameters of three isotherm models, which was presented in Table 3. The superior match with Linear isotherm model suggested the adsorption/partition mechanism between ZER molecule and NMts. According to the characterizations, organic content and hydrophobicity of NMts increased, which could improve the affinity of NMts to hydrophobic, weak polar ZER molecules since the carbon chains of OP-10 can functioned as a partition medium for ZER. However, the adsorption capacities of NMts rose from 0.5 to 1.0 CEC surfactant amount and then kept almost constant from 1.0 to 2.0 CEC level. The results seemed to be in line with the XRD change. From 0.5 to 1.0 CEC surfactant loadings, the interlayer spacing of NMts changed obviously from 0.60 to 0.88 nm, while there was only little expansion of 0.88 to 0.92 nm from 1.0 to 2.0 CEC surfactant loadings. Although the partition medium organic carbon kept increasing with surfactant loadings, the interlayer space which can hold ZER molecules did not increase linearly with surfactant loadings. The specific surface area also declined sharply when continued increasing surfactant loadings, providing less sorption sites for ZER. These findings were same with AFB_1 adsorption, demonstrating that high adsorption capacities could be achieved at a relative low surfactant loading.

3.3. Effect of pH

Generally, pH plays a critical role during mycotoxins adsorption process because feed additives firstly gather in stomach where the pH value is 3.5 and then pass through the intestine where the pH value is 6.5. The adsorption experiments of the three prepared adsorbents for both AFB_1 and ZER were compared in these two pH conditions, and the result was depicted in Fig. 8. For AFB_1, the adsorption capacity in pH of 6.5 condition was lower than that in pH of 3.5 condition, meaning that there would be a desorption when the adsorbents went through stomach to intestine. It may result from the cations in the interlayer of Mt that could be influenced by solution pH. On the other hand, solution pH also had an effect on the adsorption of ZER but the influence became smaller with increasing surfactant loadings. The little decrease in pH of 6.5 as compared to that in pH of 3.5 was due to the increased solubility of ZER in water [11]. Since more ZER molecules dissolved in water, less ZER molecules could be captured by adsorbents through hydrophobic interaction. The acid-base resistance property improved at high surfactant loadings was probably attributed to the improvement of hydrophobicity of NMts.

Table 3
The parameters of isotherm models for ZER adsorption.

ZER	Langmuir model			Freundlich model			Linear model	
	Q_{max} (mg/g)	K_L (L/mg)	R^2	K_F ($mg^{1-1/n}L^{1/n}/g$)	1/n	R^2	K_d	R^2
0.5OP-10Mt	34.36	0.05	0.4491	1.65	0.89	0.9864	1.37	0.9878
1.0OP-10Mt	68.49	0.04	0.8717	2.70	1.09	0.9892	3.17	0.9994
2.0OP-10Mt	59.88	0.05	0.9869	2.82	1.00	0.9806	2.80	0.9916

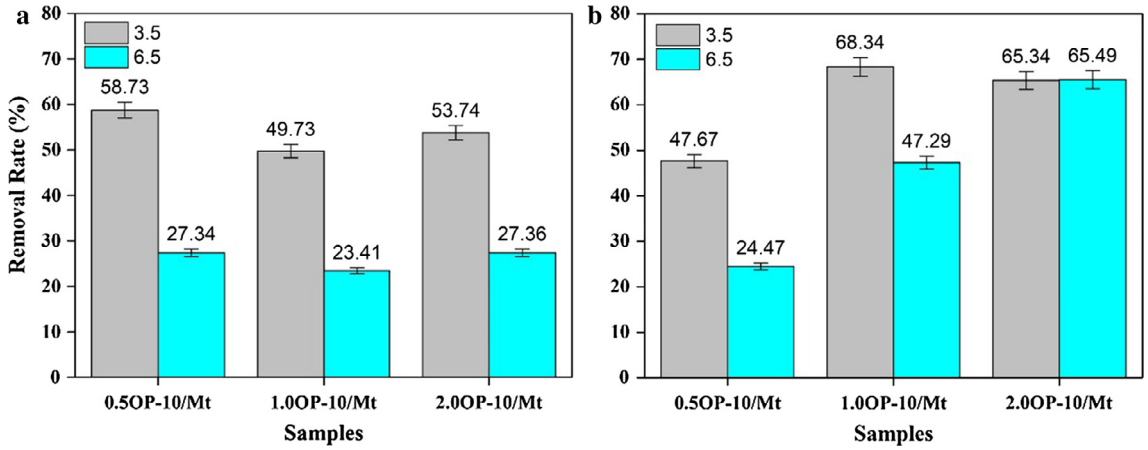


Fig. 8. Effect of pH on the adsorption performance of the prepared NMts for both (a) AFB_1 and (b) ZER. Initial concentration: 4 mg/L for AFB_1 and 16 mg/L for ZER; adsorbent amount: 0.01 g. The data points are the average values of repeat experiments. The error bars represent standard deviation of three replicates.

3.4. Comparative adsorption

Due to the fact that crops, animal feeds and foods intended for human consumption usually co-contaminated by multiple mycotoxins [42], comparative study between adsorption in single system and in binary-contaminant system was conducted to investigate the influence of one mycotoxin on the adsorption process of another mycotoxin. The result is presented in Fig. 9. Firstly, it can be seen that both AFB_1 and ZER were affected by the existence of another mycotoxin as the adsorption capacities in binary-contaminant system were lower than that in single system. However, the adsorption of ZER in binary-contaminant decreased seriously while there was only a little drop on the adsorption of AFB_1. It suggested that a competitive adsorption happened

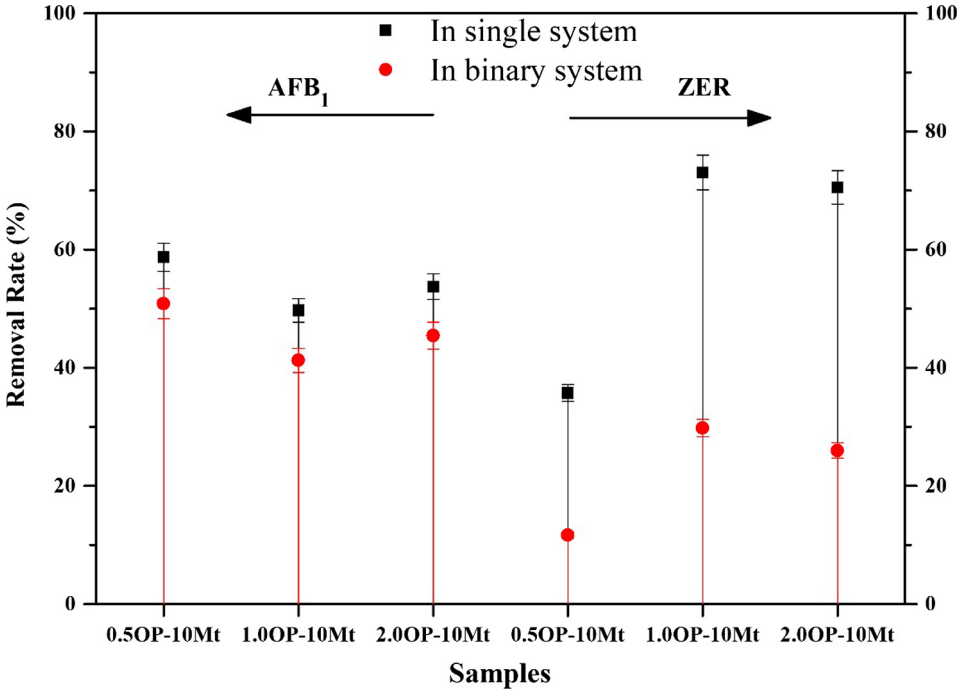


Fig. 9. Comparative study between adsorption in single system and in binary-contaminant system. Initial concentration: 4 mg/L for AFB_1 and 16 mg/L for ZER; adsorbent amount: 0.01 g. The data points are the average values of repeat experiments. The error bars represent standard deviation of three replicates.

between AFB_1 and ZER, and AFB_1 owned a stronger stability during the competitive adsorption. In Section 3.2, we proposed that the adsorption mechanism of NMts to AFB_1 were ion-dipole interaction and hydrophobic interaction, while the adsorption mechanism of NMts to ZER was hydrophobic interaction. It is known that an ion-dipole force is an attractive force that results from electrostatic attraction between an ion and a neutral molecule that has a dipole, and hydrophobic interaction is a weaken, non-covalent interaction. It seemed that the ion-dipole force was stronger than hydrophobic interaction in this study. After AFB_1 molecules were captured by NMts through ion-dipole interaction, partial sorption sites were occupied. On one hand, the adsorbed AFB_1 molecules were in favor of the adsorption of other AFB_1 molecules. On the other hand, the occupied sorption sited decreased the sorption sites for ZER.

4. Conclusion

In the current study, the potential of nonionic surfactant modified montmorillonites (NMts) as mycotoxins adsorbent was firstly evaluated by detoxification of polar aflatoxin B_1 (AFB_1) and weak polar zearalenone (ZER) from simulated gastrointestinal tract. Three NMts modified at different surfactant loadings were prepared, characterized systematically and applied for the adsorption of AFB_1 and ZER in both single and binary-contaminant systems. Two notable findings can be highlighted: (i) the modification of montmorillonite with nonionic surfactant octylphenol polyoxyethylene ether (OP-10) significantly improves the adsorption capacities of NMts to both AFB_1 and ZER, up to 2.78 and 8.54 mg/g respectively; (ii) high adsorption capacities of NMts to AFB_1 and ZER can be reached at low surfactant loadings, which would greatly save economic costs of industrial production. Compared to the recently reported mycotoxins adsorbents [43–46], most of them showed adsorption ability only to single mycotoxin, and the adsorption capacities were relatively low. These observations suggest that NMt possess tremendous potential as mycotoxins adsorbent for simultaneous detoxification of polar and non-polar mycotoxins.

Acknowledgements

The authors gratefully acknowledge the financial support provided by the National Natural Science Foundation of China (51774294), the Young Elite Scientists Sponsorship Program by CAST (2017QNRC001), the Yue Qi Young Scholar Project, China university of Mining & Technology (Beijing) and the Fundamental Research Funds for the Central Universities (2010YH10 and 2015QH01).

Appendix A. Supplementary material

Supplementary data associated with this article can be found, in the online version, at https://doi.org/10.1016/j.jcis.2018.02.020.

References

[1] C. Ji, Y. Fan, L. Zhao, Review on biological degradation of mycotoxins, Anim. Nutr. 2 (2016) 127–133.
[2] Y. Li, L. Zeng, Y. Zhou, T. Wang, Y. Zhang, Preparation and characterization of montmorillonite intercalation compounds with quaternary ammonium surfactant: adsorption effect of zearalenone, J. Nanomater. 2014 (2014) 1–7.
[3] A. Dakovic, M.T. Canovic, G.E. Rottinghaus, S. Matijasevic, Z. Sekulic, Fumonisin B_1 adsorption to octadecyldimethylbenzyl ammonium-modified clinoptilolite-rich zeolitic tuff, Micropor. Mesopor. Mat. 105 (2007) 285–290.
[4] A. Dakovic, S. Matijasevic, G.E. Rottinghaus, V. Dondur, T. Pietrass, C.F. Clewett, Adsorption of zearalenone by organomodified natural zeolitic tuff, J. Colloid Interf. Sci. 311 (2007) 8–13.
[5] R.B. Kurzel, C.L. Cetrulo, The effect of environmental pollutants on human reproduction, including birth defects, Environ. Sci. Technol. 15 (1981) 626–640.
[6] F. Kang, Y. Ge, X. Hu, C. Goikavi, M.G. Waigi, Y. Gao, W. Ling, Understanding the sorption mechanisms of aflatoxin B_1 to kaolinite, illite, and smectite clays via a comparative computational study, J. Hazard. Mater. 320 (2016) 80–87.
[7] M. Markovic, A. Dakovic, G.E. Rottinghaus, M. Kragovic, A. Petkovic, D. Krajisnik, J. Milic, M. Mercurio, B. de Gennaro, Adsorption of the mycotoxin zearalenone by clinoptilolite and phillipsite zeolites treated with cetylpyridinium surfactant, Colloids Surf. B 151 (2017) 324–332.
[8] Y. Yu, H. Wu, Y. Tang, L. Qiu, Cloning, expression of a peroxiredoxin gene from acinetobacter sp. SM04 and characterization of its recombinant protein for zearalenone detoxification, Microbiol. Res. 167 (2012) 121–126.
[9] M.A. Abdel-Wahhab, E.S. El-Denshary, A.A. El-Nekeety, K.G. Abdel-Wahhab, M. A. Hamzawy, M.F. Elyamany, N.S. Hassan, F.A. Mannaa, M.N.Q. Shaiea, R.A. Gado, M.F. Zawrah, Efficacy of organo-modified nano montmorillonite to protect against the cumulative health risk of aflatoxin B and ochratoxin A in Rats, Soft Nanosci. Let. 05 (2015) 21–35.
[10] A. Dakovic, S. Matijasevic, G.E. Rottinghaus, D.R. Ledoux, P. Butkeraitis, Z. Sekulic, Aflatoxin B_1 adsorption by natural and copper modified montmorillonite, Colloids Surf. B 66 (2008) 20–25.
[11] A. Dakovic, M.T. Canovic, V. Dondur, G.E. Rottinghaus, V. Medakovic, S. Zaric, Adsorption of mycotoxins by organozeolites, Colloids Surf. B 46 (2005) 20–25.
[12] A. Dakovic, M. Kragovic, G.E. Rottinghaus, D.R. Ledoux, P. Butkeraitis, D.Z. Vojislavljevic, S.D. Zaric, L. Stamenic, Preparation and characterization of zinc-exchanged montmorillonite and its effectiveness as aflatoxin B_1 adsorbent, Mater. Chem. Phys. 137 (2012) 213–220.
[13] J.P. Wang, F. Chi, I.H. Kim, Effects of montmorillonite clay on growth performance, nutrient digestibility, vulva size, faecal microflora, and oxidative stress in weaning gilts challenged with zearalenone, Anim. Feed Sci. Tech. 178 (2012) 158–166.
[14] Y. Zhang, R. Gao, M. Liu, B. Shi, A. Shan, B. Cheng, Use of modified halloysite nanotubes in the feed reduces the toxic effects of zearalenone on sow reproduction and piglet development, Theriogenology 83 (2015) 932–941.
[15] M. Sprynskyy, R.G. Kopciuch, K. Nowak, B. Buszewski, Removal of zearalenone toxin from synthetics gastric and body fluids using talc and diatomite: a batch kinetic study, Colloids Surf. B 94 (2012) 7–14.
[16] J. Nones, H.G. Riella, A.G. Trentin, J. Nones, Effects of bentonite on different cell types: a brief review, Appl. Clay Sci. 105–106 (2015) 225–230.
[17] S. Abbes, J.B. Salahabbes, M.M. Hetta, M. Ibrahim, M.A. Abdelwahhab, Efficacy of tunisian montmorillonite for in vitro aflatoxin binding and in vivo amelioration of physiological alterations, Appl. Clay Sci. 42 (2008) 151–157.
[18] J. Nones, H.G. Riella, N.C. Kuhnen, A. Trentin, Bentonite protects neural crest stem cells from death caused by aflatoxin B_1, Appl. Clay Sci. 104 (2015) 119–127.
[19] J.B. Dixon, I. Kannewischer, M.G. Tenorio Arvide, A.L. Barrientos Velazquez, Aflatoxin sequestration in animal feeds by quality-labeled smectite clays: an introductory plan, Appl. Clay Sci. 40 (2008) 201–208.
[20] I. Mulder, A.L. Barrientos Velazquez, M.G. Tenorio Arvide, G.N. White, J.B. Dixon, Smectite clay sequestration of aflatoxin B_1: particle size and morphology, Clays Clay Miner. 56 (2008) 558–570.
[21] M.G. Tenorio Arvide, I. Mulder, A.L. Barrientos Velazquez, J.B. Dixon, Smectite clay adsorption of aflatoxin vs. octahedral composition as indicated by FTIR, Clays Clay Miner. 56 (2008) 571–578.
[22] G. Xue, M. Gao, Z. Gu, Z. Luo, Z. Hu, The removal of p-nitrophenol from aqueous solutions by adsorption using gemini surfactants modified montmorillonites, Chem. Eng. J. 218 (2013) 223–231.
[23] R. Celis, M.C. Hermosin, J. Cornejo, Heavy metal adsorption by functionalized clays, Environ. Sci. Technol. 34 (2000) 4593–4599.
[24] C. Liu, P. Wu, Y. Zhu, L. Tran, Simultaneous adsorption of Cd^{2+} and BPA on amphoteric surfactant activated montmorillonite, Chemosphere 144 (2016) 1026–1032.
[25] J.X. Zhu, P. Zhang, Y.H. Qing, K. Wen, X.L. Su, L.Y. Ma, J.M. Wei, H.M. Liu, H.P. He, Y.F. Xi, Novel intercalation mechanism of zwitterionic surfactant modified montmorillonites, Appl. Clay Sci. 141 (2017) 265–271.
[26] H.A. Merchant, E.L. McConnell, F. Liu, C. Ramaswamy, R.P. Kulkarni, A.W. Basit, S. Murdan, Assessment of gastrointestinal pH, fluid and lymphoid tissue in the guinea pig, rabbit and pig, and implications for their use in drug development, Eur. J. Pharm. Sci. 42 (2011) 3–10.
[27] Y.H. Shen, Preparation of organobentonite using nonionic surfactants, Chemosphere 44 (2001) 989–995.
[28] B.R. Postmus, F.A.M. Leermakers, L.K. Koopal, M.A.C. Stuart, Competitive adsorption of nonionic surfactant and nonionic polymer on silica, Langmuir 23 (2007) 5532–5540.
[29] L. Huang, C. Maltesh, P. Somasundaran, Adsorption behavior of cationic and nonionic surfactant mixtures at the alumina-water interface, J. Colloid Interf. Sci. 177 (1996).
[30] P. Somasundaran, E.D. Snell, Q. Xu, Adsorption behavior of alkylarylethoxylated alcohols on silica, J. Colloid Interf. Sci. 144 (1991) 165–173.
[31] S.C. Mathur, B.M. Moudgil, Mechanisms of nonionic polymer adsorption on oxide surfaces, Miner. Metall. Proc. 15 (1998) 24–28.
[32] G. Wang, S. Wang, Z. Sun, S. Zheng, Y. Xi, Structures of nonionic surfactant modified montmorillonites and their enhanced adsorption capacities towards a cationic organic dye, Appl. Clay Sci. 148 (2017) 1–10.

[33] Z. Sun, Y. Park, S. Zheng, G.A. Ayoko, R.L. Frost, XRD, TEM, and thermal analysis of Arizona Ca-montmorillonites modified with didodecyldimethylammonium bromide, J. Colloid Interf. Sci. 408 (2013) 75–81.
[34] Z. Sun, Y. Park, S. Zheng, G.A. Ayoko, R.L. Frost, Thermal stability and hot-stage Raman spectroscopic study of Ca-montmorillonite modified with different surfactants: a comparative study, Thermochim. Acta 569 (2013) 151–160.
[35] S. Brunauer, L.S. Deming, W.E. Deming, E. Teller, On a theory of the van der waals adsorption of gases, J. Am. Chem. Soc. 62 (1940) 1723–1732.
[36] Y. Park, G.A. Ayoko, E. Horvath, R. Kurdi, J. Kristof, R.L. Frost, Structural characterisation and environmental application of organoclays for the removal of phenolic compounds, J. Colloid Interf. Sci. 393 (2013) 319–334.
[37] J. Xu, L. Wang, Y. Zhu, Decontamination of bisphenol A from aqueous solution by graphene adsorption, Langmuir 28 (2012) 8418–8425.
[38] A.J. Ramos, E. Hernandez, In vitro aflatoxin adsorption by means of a montmorillonite silicate. A study of adsorption isotherms, Anim. Feed Sci. Tech. 62 (1996) 263–269.
[39] Y. Deng, A.L.B. Velazquez, F. Billes, J.B. Dixon, Bonding mechanisms between aflatoxin B_1 and smectite, Appl. Clay Sci. 50 (2010) 92–98.
[40] Y. Deng, M. Szczerba, Computational evaluation of bonding between aflatoxin B_1 and smectite, Appl. Clay Sci. 54 (2011) 26–33.
[41] T.D. Phillips, A.B. Sarr, P.G. Grant, Selective chemisorption and detoxification of aflatoxins by phyllosilicate clay, Nat. Toxins 3 (1995) 204–213.
[42] M.I. Almeida, N.G. Almeida, K.L. Carvalho, G.A. Goncalves, C.N. Silva, E.A. Santos, J.C. Garcia, E.A. Vargas, Co-occurrence of aflatoxins B(1), B(2), G(1) and G(2), ochratoxin A, zearalenone, deoxynivalenol, and citreoviridin in rice in Brazil, Food Addit. Contam. A 29 (2012) 694–703.
[43] X.J. Bai, C.P. Sun, J. Xu, D. Liu, Y.Y. Han, S.L. Wu, X.H. Luo, Detoxification of zearalenone from corn oil by adsorption of functionalized GO systems, Appl. Surf. Sci. 430 (2018) 198–207.
[44] M. Sprynskyy, I.K. Konieczka, R.G. Kopciuch, B. Buszewski, Separation of aflatoxin B_1 from synthetic physiological fluids using talc and diatomite: kinetic and isotherm aspects, J. Chromatogr. B 1072 (2018) 1–8.
[45] J. Nones, A. Solhaug, G.S. Eriksen, D.L.P. Macuvele, A. Poli, C. Soares, A.G. Trentin, H.G. Riella, J. Nones, Bentonite modified with zinc enhances aflatoxin B_1 adsorption andincrease survival of fibroblasts (3T3) and epithelial colorectaladenocarcinoma cells (Caco-2), J. Hazard. Mater. 337 (2017) 80–89.
[46] F.B. Taheur, K. Fedhila, K. Chaieb, B. Kouidhi, A. Bakhrouf, L. Abrunhosa, Adsorption of aflatoxin B1, zearalenone and ochratoxin A by microorganisms isolated from Kefir grains, Int. J. Food Microbiol. 251 (2017) 1–7.